Table 3 Regions showing significant difference in BP_{ND} between low/middle- and high-education groups in the voxel-based analysis

Comparison	Region	BA	MNI coordinates (*x*, *y*, *z*)	voxels	*t*-value
Education high > education low/middle	None				
Education high < education low/middle	R supramarginal gyrus	40	50, −36, 32	647	4.89
	L lingual gyrus	18	−16, −78, 2	462	4.85
	L middle frontal gyrus	11	−22, 38, −10	129	4.56
	R putamen	—	32, −18, −4	458	4.48
	R inferior frontal gyrus	47	44, 20, 20	56	4.25
	L superior parietal gyrus	7	−28, −44, 42	59	4.13
	L hippocampus	—	−40, −20, −10	217	4.04
	R middle frontal gyrus	11	18, 44, −14	82	4.04
	L inferior parietal gyrus	40	−48, −20, 24	170	4.03
	R inferior parietal gyrus	40	42, −28, 52	132	3.93
	R thalamus	—	24, −32, 2	75	3.85
	L middle temporal gyrus	37	−40, −64, 0	83	3.81
	L putamen	—	−30, 6, −2	74	3.80

BP_{ND}, binding potential; MNI, Montreal Neurological Institute; BA, Brodmann area; R, right; L, left.

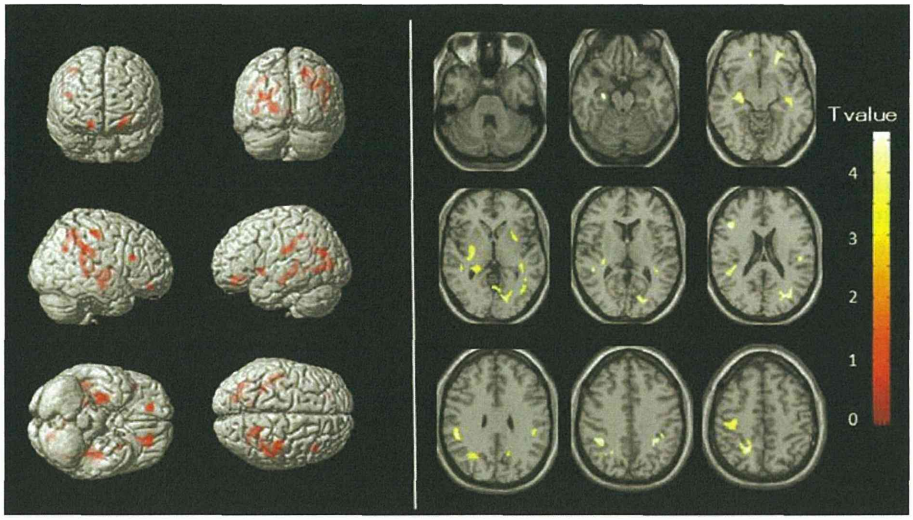

Figure 2 Images of voxel-based maps showing greater Pittsburgh Compound B-binding potential (BP_{ND}) values in the low/middle-education group compared with the highly educated group ($p < 0.001$, uncorrected, extent threshold >50 voxels). Rendered images are on the left, and axial images are on the right. The Montreal Neurological Institute coordinates of the areas showing significantly higher BP_{ND} values in the low/middle-education group compared with the high-educated group are shown in Table 3.

general intelligence. We found a higher RCPM score in the highly educated group, and the difference in the sex ratio between the groups was nearly significant. However, the finding of higher cortical PIB-BP_{ND} values in the participants with less education was not affected by the inclusion of the possible confounding variables of sex, age, or RCPM scores. In addition, we found a significant correlation between the duration of education and PIB binding in all of the subjects.

The lower incidence of AD in highly educated populations has been shown in several epidemiological studies (Stern *et al.*, 1994), but the protective mechanism of education against the disease is still unclear. Our findings indicated reduced amyloid pathology in highly educated and cognitively normal participants, which leads to the proposal that early-life education is associated with PIB, suggesting that it may have an inhibitory effect on AD pathology. Our study analyzes the effects of education on the development of pathological changes in the brain during the presymptomatic phase of AD.

One explanation for the negative relationship between early-life education and AD pathology was that it was induced from psychosocial factors, such as socioeconomic and lifestyle differences. For example, higher education is often associated with a healthier

lifestyle, less disease, and lower exposure to toxic factors due to a better environment. These may contribute to the differences between the educational groups, as has been suggested for heart disease mortality (Springer *et al.*, 2005). Another possibility is that lifelong mental stimulation results from education. We expected that people with higher education had more knowledge and opportunities for various experiences. They could have an inquiring mind and have a greater chance for developing their imagination and intelligence. As a result, they may have lifelong cognitive stimulation that induces high neural activity.

Recent *in vitro* studies in animals and humans have indicated that neural activity regulates the secretion of Aβ (Kamenetz *et al.*, 2003; Cirrito *et al.*, 2005; Brody *et al.*, 2008; Bero *et al.*, 2011). Although it is difficult to verify the association between increased neural activation and Aβ deposition in humans, individuals with greater early- and middle-life cognitive activity have been shown to have lower [^{11}C]PIB uptake in a previous study (Landau *et al.*, 2012). Individuals who participate in a variety of cognitively stimulating activities during their lifespan may develop more efficient neural processing that results in less Aβ deposition (Jagust and Mormino, 2011). Supporting this idea, transgenic Aβ-expressing mice that were exposed to enriched environments deposit less Aβ than control animals (Lazarov *et al.*, 2005; Costa *et al.*, 2007).

Our study had some limitations. Firstly, in contrast to the epidemiologic data rested on large population studies, our data of 30 individuals recruited from the local area by poster advertisement are not based on the random sampling selection. Secondly, this was a cross-sectional survey and not a longitudinal follow-up study. Thirdly, some of the subjects in the low/middle-education group showed high BP_{ND} values and could not be regarded as healthy subjects, even though they were cognitively normal. It would be premature to draw definitive conclusions from this analysis. However, in spite of these shortcomings, the current data would be useful as pilot for future studies in a larger, more representative cohort.

The present study possibly extends previous findings of a lower incidence of AD in highly educated populations, suggesting that education provides protection against the disease. Our findings are not opposed to the brain reserve hypothesis, which implies that people with higher education have a greater reserve capacity. People with more education might be prone to have a greater inhibitory effect against Aβ deposition before the preclinical stage and, at the same time, have greater reserve capacity: requiring greater pathological changes for dementia to manifest.

Conflict of interest

None declared.

Key points

- Reduced amyloid pathology in highly educated, cognitively normal subjects.
- Early-life education has a negative association with AD pathology in the later stage of life.

Acknowledgements

This research was supported by the Grants-in-Aid for Scientific Research (C) 24591740 and 24591708 from the Japan Society for the Promotion of Science and by the Health and Labour Sciences Research Grants for Research on Dementia (H25-01). The authors have no proprietary interest or any conflict of interest related to this study.

References

Arenaza-Urquijo EM, Landeau B, La Joie R, *et al.* 2013. Relationships between years of education and gray matter volume, metabolism and functional connectivity in healthy elders. *Neuroimage* **83**: 450–457.

Bennett DA, Schneider JA, Arvanitakis Z, *et al.* 2006. Neuropathology of older persons without cognitive impairment from two community-based studies. *Neurology* **66**: 1837–1844.

Bero AW, Yan P, Roh JH, *et al.* 2011. Neuronal activity regulates the regional vulnerability to amyloid-β deposition. *Nat Neurosci* **14**: 750–756.

Brody DL, Magnoni S, Schwetye KE, *et al.* 2008. Amyloid-beta dynamics correlate with neurological status in the injured human brain. *Science* **321**: 1221–1224.

Cirrito JR, Yamada KA, Finn MB, *et al.* 2005 Synaptic activity regulates interstitial fluid amyloid-beta levels in vivo. *Neuron* **48**: 913–922.

Costa DA, Cracchiolo JR, Bachstetter AD, *et al.* 2007. Enrichment improves cognition in AD mice by amyloid-related and unrelated mechanisms. *Neurobiol Aging* **28**: 831–844.

Dubois B, Slachevsky A, Litvan I, Pillon B. 2000. The FAB: a Frontal Assessment Battery at bedside. *Neurology* **55**: 1621–1626.

Folstein MF, Folstein SE, McHugh PR. 1975. "Mini-mental state". A practical method for grading the cognitive state of patients for the clinician. *J Psychiatr Res* **12**: 189–198.

Hoffman EJ, Huang SC, Phelps ME. 1979. Quantitation in positron emission computed tomography: 1. Effect of object size. *J Comput Assist Tomogr* **3**: 299–308.

Innis RB, Cunningham VJ, Delforge J, *et al.* 2007. Consensus nomenclature for in vivo imaging of reversibly binding radioligands. *J Cereb Blood Flow Metab* **27**: 1533–1539.

Jagust WJ, Mormino EC. 2011. Lifespan brain activity, β-amyloid, and Alzheimer's disease. *Trends Cogn Sci* **15**: 520–526.

Kamenetz F, Tomita T, Hsieh H, *et al.* 2003. APP processing and synaptic function. *Neuron* **37**: 925–937.

Kemppainen NM, Aalto S, Wilson IA, *et al.* 2006. Voxel-based analysis of PET amyloid ligand [^{11}C]PIB uptake in Alzheimer disease. *Neurology* **67**: 1575–1580.

Kemppainen NM, Aalto S, Wilson IA, *et al.* 2007. PET amyloid ligand [^{11}C]PIB uptake is increased in mild cognitive impairment. *Neurology* **68**: 1603–1606.

Klunk WE, Engler H, Nordberg A, *et al.* 2004. Imaging brain amyloid in Alzheimer's disease with Pittsburgh Compound-B. *Ann Neurol* **55**: 306–319.

Landau SM, Marks SM, Mormino EC, *et al.* 2012. Association of lifetime cognitive engagement and low β-amyloid deposition. *Arch Neurol* **69**: 623–629.

Lazarov O, Robinson J, Tang YP, *et al.* 2005. Environmental enrichment reduces Abeta levels and amyloid deposition in transgenic mice. *Cell* **120**: 701–713.

Logan J, Fowler JS, Volkow ND, *et al.* 1996. Distribution volume ratios without blood sampling from graphical analysis of PET data. *J Cereb Blood Flow Metab* **16**: 834–840.

Lopresti BJ, Klunk WE, Mathis CA, *et al.* 2005. Simplified quantification of Pittsburgh Compound B amyloid imaging PET studies: a comparative analysis. *J Nucl Med* **46**: 1959–1972.

Müller-Gärtner HW, Links JM, Prince JL, *et al.* 1992. Measurement of radiotracer concentration in brain gray matter using positron emission tomography: MRI-based correction for partial volume effects. *J Cereb Blood Flow Metab* **12**: 571–583.

Morris JC, Roe CM, Xiong C, *et al.* 2010. APOE predicts amyloid-beta but not tau Alzheimer pathology in cognitively normal aging. *Ann Neurol* **67**: 122–131.

Partington JE, Leiter RG. 1949. Partington's pathway test. *Psychol Serv Cent Bull* **1**: 9–20.

Pike KE, Savage G, Villemagne VL, *et al.* 2007. Beta-amyloid imaging and memory in non-demented individuals: evidence for preclinical Alzheimer's disease. *Brain* **130**: 2837–2844.

Price JC, Klunk WE, Lopresti BJ, *et al.* 2005. Kinetic modeling of amyloid binding in humans using PET imaging and Pittsburgh Compound-B. *J Cereb Blood Flow Metab* **25**: 1528–1547.

Raven JC. 1958. Guide to the Standard Progressive Matrices. HK Lewis: London.

Rentz DM, Locascio JJ, Becker JA, *et al.* 2010. Cognition, reserve, and amyloid deposition in normal aging. *Ann Neurol* **67**: 353–364.

Rosen WG, Mohs RC, Davis KL. 1984. A new rating scale for Alzheimer's disease. *Am J Psychiatry* **141**: 1356–1364.

Spreen O, Strauss E. 1991. A Conpendium of Neuropsychological Tests. Oxford University Press: Oxford.

Springer MV, McIntosh AR, Winocur G, Grady CL. 2005. The relation between brain activity during memory tasks and years of education in young and older adults. *Neuropsychology* **19**: 181–192.

Stern Y. 2006. Cognitive reserve and Alzheimer disease. *Alzheimer Dis Assoc Disord* **20**: S69-74.

Stern Y, Gurland B, Tatemichi TK, *et al.* 1994. Influence of education and occupation on the incidence of Alzheimer's disease. *JAMA* **271**: 1004–1010.

Vemuri P, Lesnick TG, Przybelski SA, *et al.* 2012. Effect of lifestyle activities on Alzheimer disease biomarkers and cognition. *Ann Neurol* **72**: 730–738.

Wechsler D. 1987. Wechsler Memory Scale-Revised. Harcourt Brace Jovanovich: San Antonio.

Wirth M, Villeneuve S, La Joie R, Marks SM, Jagust WJ 2014 Gene-environment interactions: lifetime cognitive activity, APOE genotype, and β-amyloid burden. *J Neurosci* **34**: 8612–8617.

Yasuno F, Hasnine AH, Suhara T, *et al.* 2002. Template-based method for multiple volumes of interest of human brain PET images. *Neuroimage* **16**: 577–586.

Yesavage JA, Brink TL, Rose TL, *et al.* 1982–1983. Development and validation of a geriatric depression screening scale: a preliminary report. *J Psychiatr Res* **17**: 37–49.

Clinical & Cellular Immunology

Yasuno et al., J Clin Cell Immunol 2014, 5:3
http://dx.doi.org/10.4172/2155-9899.1000221

Research Article Open Access

Possible Protective Effect of Regulatory T cells on White Matter Microstructural Abnormalities in Stroke Patients

Fumihiko Yasuno[1,2*], Akihiko Taguchi[3,4], Akie Kikuchi-Taura[5], Akihide Yamamoto[2], Hiroaki Kazui[6], Takashi Kudo[6], Atsuo Sekiyama[7], Katsufumi Kajimoto[3], Toshihiro Soma[5], Toshifumi Kishimoto[1], Hidehiro Iida[2] and Kazuyuki Nagatsuka[3]

[1]*Department of Neuropsychiatry, Nara Medical University, Kashihara, Japan*

[2]*Department of Investigative Radiology, National Cerebral and Cardiovascular Center, Suita, Japan*

[3]*Department of Neurology, National Cerebral and Cardiovascular Center, Suita, Japan*

[4]*Institute of Biomedical Research and Innovation, Foundation for Biomedical Research and Innovation, Kobe, Japan*

[5]*Division of Hematology, Department of Internal Medicine, Hyogo College of Medicine, Nishinomiya, Japan*

[6]*Department of Neuropsychiatry, Osaka University Medical School, Suita, Japan*

[7]*Department of Brain Science, Osaka City University Graduate School of Medicine, Osaka, Japan*

***Corresponding author:** Fumihiko Yasuno, M.D., Ph.D., Department of Psychiatry, Nara Medical University, 840 Shijocho, Kashihara, Nara, 634-8522, Japan, Tel: +81-744-22-3051; Fax: +81-744-22-3854. E-mail: ejm86rp@yahoo.co.jp

Received date: April 20, 2014, **Accepted date:** June 02, 2014, **Published date:** June 09, 2014

Abstract

Background: Despite advances in the understanding of stroke, therapeutic options for stroke are limited. Inflammatory mechanisms activated after brain ischemia are a key target of translational cerebrovascular research. The purpose of the present study was to investigate the existence of microstructure abnormalities in the white matter of stroke patients and their relationship to lymphocyte subsets.

Methods: The study included 18 patients with acute ischemic stroke and 22 healthy subjects. Diffusion tensor scans with magnetic resonance imaging were performed. Whole brain voxel-based analysis was used to compare fractional anisotropy (FA) in the stroke and healthy control groups. Blood samples were obtained from all subjects at the initial examination. The lymphocyte subsets in peripheral blood were evaluated with flow cytometric analysis. Helper T cells ($CD3^+$ and $CD4^+$), cytotoxic T cells ($CD3^+$ and $CD8^+$), B cells ($CD19^+$), natural killer cells ($CD16^+$ or $CD56^+$), and regulatory T cells (T_{regs}) ($CD4^+$, $CD25^+$, and $FOXP3^+$) were identified.

Results: In the voxel-based analysis, FA in the bilateral anterior limbs of the internal capsule was lower in stroke patients than in healthy subjects. These regions exhibited decreased axial diffusivity. The frequency of T_{regs} was lower in patients than in healthy controls. In patients, we found a significant positive relationship between the level of circulating T_{regs} and the FA value in the anterior limb of the internal capsule.

Conclusions: Patients exhibited a decreased frequency of circulating T_{regs} and the degree of reduction correlated with the decrease in the FA value in the internal capsule. T_{regs} might attenuate post-stroke white matter tissue damage by limiting the immune response. Our findings demonstrate the need for further study of the role of T_{regs} in the prevention of post-stroke cerebral damage.

Keywords: Stroke; Magnetic resonance imaging (MRI); Diffusion tensor imaging (DTI); Fractional anisotropy (FA); Regulatory T lymphocyte (T_{reg})

Introduction

Stroke is the third leading cause of death and the most frequent cause of permanent disability in adults worldwide [1]. Despite considerable advances in understanding the pathophysiology of cerebral ischemia, therapeutic options for stroke are limited. Inflammatory mechanisms activated after brain ischemia are a key target of current translational cerebrovascular research. Stoke induces a profound local inflammatory response involving various types of immune cells that transmigrate across the activated blood-brain barrier to invade the brain [2].

In the search for ways to prevent cerebral damage due to stroke, several factors related to inflammation have received considerable attention [3-5]. In particular, T lymphocytes are central to the development of a sustained inflammatory response in brain injury after a stroke. T cells are sources of pro-inflammatory cytokines and cytotoxic substances, such as reactive oxygen species, that likely contribute to neuronal death and poor outcome in stroke. However, recent evidence has indicated a novel role of T cells in promoting brain tissue repair and regeneration in the weeks and months after a stroke [6]. The complex role of T lymphocytes in ischemic stroke remains poorly understood. Further research is needed to understand which T-cell subpopulations produce and prevent damage after a stroke.

The primary aim of the present study was to elucidate the microstructural abnormalities in the white matter circuit in stroke patients and determine their relationship to the levels of circulating T lymphocytes. To identify microstructural abnormalities in stroke

patients, diffusion tensor imaging was performed and whole brain voxel-based analysis was used to compare fractional anisotropy (FA) in acute ischemic stroke patients and healthy control subjects. Furthermore, the circulating T-cell subpopulations in stroke patients and healthy subjects were compared, and the association between T-cell subpopulations and white matter microstructural abnormalities in patients was assessed.

Methods

Subjects

After providing subjects with a complete description of the study, written informed consent was obtained. The study was approved by the medical ethics committee of the National Cerebral and Cardiovascular Center of Japan. The patients were of Japanese ethnicity and were recruited from the neurology unit of the National Cerebral and Cardiovascular Center hospital. The patients had initially been hospitalized for treatment of acute ischemic stroke.

Stroke was diagnosed by neurologists according to the WHO criteria (1989). After the assessment, a group of psychiatrists and neurologists reviewed the data and reached a consensus regarding the presence or absence of psychiatric disease, including dementia, according to DSM-IV criteria. Patients were included if they met the following criteria: 1) a focal lesion of either the right or left hemisphere on magnetic resonance imaging (MRI); 2) absence of other neurologic, neurotoxic, and metabolic conditions; 3) modest ischemic insult (modified Rankin scale ≤ 4) with absence of a significant verbal comprehension deficit; and 4) occurrence of stroke 10–28 days before the examinations. The exclusion criteria were: 1) transient ischemic attack, cerebral hemorrhage, subdural hematoma, or subarachnoid hemorrhage; 2) history of a central nervous system disease such as tumor, trauma, hydrocephalus, or Parkinson's disease; and 3) pre-stroke history of depression. Eighteen subjects participated in the MRI study and the analysis of lymphocyte subsets in peripheral blood.

Twenty-two healthy control subjects were recruited for this study from the local area by poster advertisement. Subjects were excluded if they had a history or current diagnosis of any DSM-IV axis I or neurological illness. The major characteristics of this cohort are summarized in Table 1.

Characteristic	Stroke patients (n = 18)	Healthy control subjects (n = 22)	t or χ^2	p
Age (years)	70.0 ± 6.7	67.2 ± 5.5	t=1.46	0.15
Female, n (%)	4 (22.2)	8 (36.3)	χ^2=0.94	0.33
MMSE score	28.4 ± 1.9	29.3 ± 1.0	t=1.98	0.06
History of disease, n (%)				
Diabetes mellitus	5 (27.8)	2 (9.1)	χ^2_1=2.40	0.12
Hyperlipidemia	5 (27.8)	1 (4.5)	χ^2_1=4.19	0.04*
Hypertension	14 (77.8)	5 (22.7)	χ^2_1=12.0	<0.01**
Fazekas DWMH score, n (%)				
0–2	11 (61.1)	22 (100)		
3	7 (38.9)	0 (0.0)	χ^2=10.4	<0.01**
Fazekas PVH score, n (%)				
0–2	13 (72.2)	22 (100)		
3	5 (27.8)	0 (0.0)	χ^2=6.98	<0.01**
mRS score	1.9 ± 0.7	-		
NIHSS score	2.8 ± 0.9	-		
Anti-coagulant/platelet medication, n (%)				
Warfarin	3 (16.7)			
Acetylsalicylic acid	13 (72.2)			
Clopidogrel sulfate	2 (11.1)			
Cilostazol	3 (16.7)			
Number of acute infarcts	1.2 ± 0.5	-		
Volume of acute infarcts (mL)	1.6 ± 0.9	-		
Acute infarct location, n (%)				
Basal ganglia	11 (61.1)	-		
Subcortical white matter	6 (33.3)			
Thalamus	1 (5.6)	-		
Laterality of acute hemisphere infarcts				
Left hemisphere, n (%)	9 (50.0)	-		

Data are the mean ± SD. * p < 0.05, ** p < 0.01; MMSE: Mini-Mental State Examination; DWMH: Deep White Matter Hyperintensity; PVH: Periventricular Hemorrhage; mRS: Modified Rankin Scale; NIHSS: National Institutes of Health Stroke Scale

Table 1: Demographic characteristics of patients and healthy control subjects.

All patients received a neurological examination (modified Rankin Scale (mRS) [7], National Institutes of Health Stroke Scale (NIHSS) [8]) on the day of the MRI scan. Cognitive function was measured with the mini-mental state examination (MMSE) [9] in patients and control subjects. MRIs were conducted for all of the study subjects. The severity of white matter hyper intensity (WMH) was classified using the Fazekas scale, which is a simple visual rating scale used to rate the degree of leukoaraiosis (WMH). It provides an assessment of WMH in the peri-ventricular area (PVH) and in deep white matter (DWMH) on a four-point scale (0–3) [10].

MRI data acquisition

All MRI examinations were performed using a 3-Tesla whole-body scanner (Signa Excite HD V12M4; GE Healthcare, Milwaukee, WI, USA) with an 8-channel phased-array brain coil. Diffusion tensor images were acquired with a locally modified single-shot echo-planar imaging sequence by using parallel acquisition at a reduction (ASSET) factor of 2 in the axial plane. Imaging parameters were as follows: Repetition Time (TR)=17 seconds; Eco Time (TE)=72 ms; b=0 and

1000 seconds/mm^2; acquisition matrix, 128 × 128; field of view (FOV), 256 mm; section thickness, 2.0 mm; no intersection gap; 74 sections. The reconstruction matrix was the same as the acquisition matrix, and 2 mm × 2 mm × 2 mm isotropic voxel data were obtained. A motion probing gradient was applied in 55 directions, and 4144 images were obtained. The acquisition time was 15 min 52 seconds.

To reduce blurring and signal loss arising from field in homogeneity, an automated high-order shimming method based on spiral acquisitions [11] was used before acquiring diffusion tensor imaging scans. FMRIB software (FMRIB Center, Department of Clinical Neurology, University of Oxford, Oxford, England; http://www.fmrib.ox.ac.uk/fsl/) was used to correct for motion and distortion from eddy current and B0 in homogeneity. B0 field mapping data were also acquired with the echo time shift (2.237 msec) method based on two gradient echo sequences.

High-resolution, three-dimensional T1-weighted images were acquired using a spoiled gradient-recalled sequence (TR=12.8 msec; TE=2.6 msec; flip angle=8°; FOV, 256 mm; 188 sections in the sagittal plane; acquisition matrix, 256 × 256; acquired resolution, 1 × 1 × 1 mm). T2-weighted images were obtained using a fast-spin echo (TR=4800 ms; TE=101 ms; echo train length (ETL)=8; FOV=256 mm; 74 slices in the transverse plane; acquisition matrix, 160 × 160; acquired resolution, 1 × 1 × 2 mm).

Image processing

Fractional anisotropy maps, diffusion weighted images, and three eigen values (λ1, λ2, and λ3) were generated for each individual using FMRIB software. First, brain tissue was extracted using the Brain Extraction Tool. Brain maps for each of the 55 directions were eddy-corrected. Subsequently, FA values were calculated at each voxel using the FSL FMRIB Diffusion Toolbox.

Image preprocessing and statistical analysis were carried out using SPM8 software (Welcome Department of Imaging Neuroscience, London, England). Each subject's echo planar image was spatially normalized to the Montreal Neurological Institute echo planar image template using parameters determined from the normalization of the image with a b value of 0 seconds/mm^2. Images were resampled with a final voxel size of 2 × 2 × 2 mm^3. Normalized maps were spatially smoothed using an isotropic Gaussian filter (8-mm full-width at half-maximum).

Voxel-based analysis

Voxel-based analysis was performed using SPM8 software. FA maps of patients and healthy subjects were compared using analysis of covariance (ANCOVA), with age and sex as covariates. Statistical inferences were made with a voxel-level threshold of $p<0.001$, uncorrected, and a minimum cluster size of 100 voxels. The regional FA value was calculated by averaging the FA values for all voxels within the volume of interest (VOI), corresponding to the cluster composed of significant contiguous voxels in the above analysis. The same VOIs were applied to λ_1 - λ_3 images, and λ_1 - λ_3 values were extracted. Axial (λ_1) and radial diffusivity ($[\lambda_2 + \lambda_3]/2$) were compared.

Flow cytometric analysis of lymphocyte subsets in peripheral blood

Blood samples (5 mL) were obtained from all patients and healthy control subjects at the initial examination. The samples were collected into tubes containing sodium heparin. Peripheral blood mononuclear cells (PBMCs) were isolated using a Ficoll density gradient (Ficoll-Paque PLUS; GE Healthcare Bio-Sciences AB, Uppsala, Sweden) according to the manufacturer's protocol. PBMCs were washed twice with phosphate buffered saline containing 1% fetal calf serum and 2 mM ethylene diamine tetra acetate.

To identify helper T cells ($CD3^+$ and $CD4^+$), cytotoxic T cells ($CD3^+$ and $CD8^+$), B cells ($CD19^+$), and natural killer (NK) cells ($CD16^+$ or $CD56^+$), the PBMCs were incubated with fluorescein isothiocyanate (FITC)-conjugated anti-human CD3 (Beckman Coulter, Orange Country, CA, USA), phycoerythrin-cyanin 5 (PC5)-conjugated anti-human CD4 (Beckman Coulter), phycoerythrin-cyanin 7 (PC7)-conjugated anti-human CD8 (Beckman Coulter), phycoerythrin (PE)-conjugated anti-human CD19 (Beckman Coulter), PC5-conjugated anti-human CD16 (Beckman Coulter), and/or PE-conjugated anti-human CD56 (Beckman Coulter) at 4°C for 20 min. To identify T_{regs} ($CD4^+$, $CD25^+$, and $FOXP3^+$), PBMCs were incubated with FITC-conjugated anti-human CD4 (Beckman Coulter) and PC5-conjugated anti-human CD25 (Beckman Coulter) at 4°C for 20 min. After surface staining, PBMCs were fixed, permeabilized, and stained with PE-conjugated anti-human FOXP3 (Becton Dickinson, Franklin Lakes, NJ, USA) according to the manufacturer's instructions. As negative controls, fluorochrome-conjugated non-specific isotype-matched antibodies (Beckman Coulter) were used. Stained cells were analyzed using a FC500 cytometer and CXP software (Beckman Coulter). The percentage of cells stained with a particular antibody was reported after subtracting the percentage of cells stained with the relevant negative isotype control antibodies.

Statistical analysis

Group differences in the demographic characteristics of patients and healthy controls were examined with an unpaired t-test and Pearson's χ^2 test. To examine group differences in FA values and axial/radial diffusivity in VOIs from the voxel-based analysis, we performed ANCOVA with age and sex as covariates.

We also used ANCOVA with age and sex as covariates to examine differences in the percentage of helper T cells, cytotoxic T cells, regulatory T cells, B cells, and NK cells between patients and healthy controls. For cells that showed significant differences between groups, the correlation between the FA values and the percentage of cells was examined using Spearman's correlation analysis.

All statistical tests were two-tailed and reported at $p<0.05$. The Bonferroni correction was applied to avoid type I errors due to the multiplicity of statistical analyses. Statistical analysis of the data was performed using SPSS for Windows 19.0 (IBM Japan Inc., Tokyo, Japan).

Results

Demographic and clinical data

Table 1 summarizes the demographic and clinical characteristics of the study subjects. Patients did not differ significantly from healthy control subjects in age, sex, or MMSE scores. The occurrence of hyperlipidemia and hypertension was significantly higher in patients than in healthy controls. There were no healthy control subjects with Fazekas scores higher than 3. Table 1 also shows the mRS and NIHSS scores, treatment with anti-coagulant/platelet medication, and the location and volume of the infarct. Patients exhibited some disability

from stroke at the time of the examination. All patients took anti-coagulant and/or anti-platelet medicine. Infarction occurred in the basal ganglia (61.1%), sub-cortical white matter (33.3%), and thalamus (5.6%). There was no significant laterality of hemisphere infarcts. Representative MR images of patients and controls are shown in Figure 1.

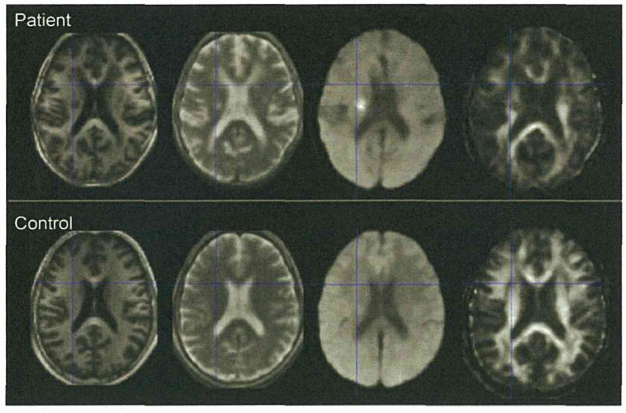

Figure 1: Representative MR images for patients and controls T1-weighted, T2-weighted, diffusion weighted, and fractional anisotropic (FA) images are shown, respectively, from left to right. All figures were spatially normalized to the image template in SPM8, and the axial slices are shown (z=18). The vertical and horizontal lines in the images represent the coordinates of x=-26 and y=12, respectively.

FA values in patient and control groups

In the voxel-based analysis of FA values, the white matter FA values in the left and right anterior limbs of the internal capsule differed in the patient and healthy control groups [left anterior limb of internal capsule: (x, y, z)=(-26,12,18), cluster voxel size=831, T=5.20; right anterior limb of internal capsule: (x,y,z)=(26,16,4), cluster voxel size=487, T=5.24] (Figure 2A). Figure 2B shows scatter plots of the FA values of the anterior limb of the internal capsule. Table 2 shows the FA values and radial/axial diffusivity in the affected regions. Decreased axial diffusivity, but no change in radial diffusivity, was observed in the affected regions.

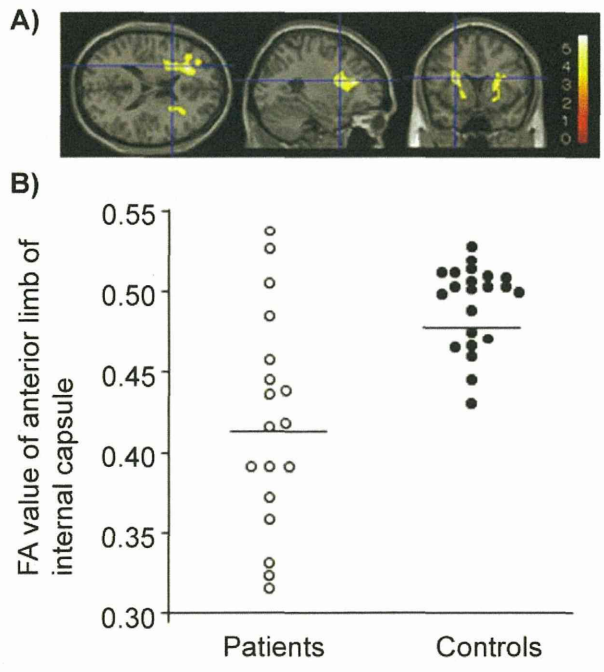

Figure 2: White matter fractional anisotropy (FA) in stroke patients and control subjects. (A) Voxel-based analysis was performed using SPM8 software. FA maps of patients (n=18) and healthy subjects (n=22) were compared using analysis of covariance (ANCOVA), with age and sex as covariates. Statistical inferences were made with a voxel-level threshold of $p<0.001$, uncorrected, and a minimum cluster size of 100 voxels. Statistical parametric mapping projections were superimposed on a representative magnetic resonance image (x=-26, y=12, z=18). FA in the right and left anterior limbs of the internal capsule was reduced in stroke patients. **(B)** Scatter plots of FA values in the regions of FA reduction in stroke patients. The regional FA value was calculated by averaging the FA values for all voxels within the volume of interest corresponding to the cluster composed of significant contiguous voxels in the preceding analysis. In the bilateral anterior limbs of the internal capsule, the FA values of stroke patients were lower than those of healthy subjects ($p<0.01$).

			Analysis of covariance †	
FA and axial/radial diffusivity	**Stroke patients (n=18)**	**Healthy controls (n=22)**	**F (1, 36)**	**p**
Left anterior limb of internal capsule				
FA	0.41 ± 0.08	0.48 ± 0.03	16.4	<0.001**
Axial diffusivity ($\times 10^{-3}$)	4.16 ± 0.32	4.37 ± 0.30	4.24	0.05 *
Radial diffusivity ($\times 10^{-3}$)	3.96 ± 0.30	4.04 ± 0.29	0.48	0.49
Right anterior limb of internal capsule				
FA	0.43 ± 0.06	0.50 ± 0.03	23.0	<0.001**

Axial diffusivity ($\times 10^{-3}$)	4.14 ± 0.33	4.35 ± 0.30	4.03	0.05
Radial diffusivity ($\times 10^{-3}$)	3.93 ± 0.31	4.01 ± 0.30	0.46	0.50
Bilateral anterior limbs of internal capsule				
FA	0.42 ± 0.07	0.49 ± 0.03	20.6	<0.001**
Axial diffusivity ($\times 10^{-3}$)	4.15 ± 0.32	4.36 ± 0.30	4.15	0.05 *
Radial diffusivity ($\times 10^{-3}$)	3.95 ± 0.30	4.02 ± 0.29	0.47	0.50
† Age and sex were entered as covariates; Data are the mean ± SD. * $p < 0.05$, ** $p < 0.01$; FA: Fractional Anisotropy; VOI: Volume of Interest				

Table 2: FA values and axial/radial diffusivity in the VOI in patients and healthy control subjects.

			Analysis of covariance †	
	Stroke patients (n=18)	**Healthy controls (n=22)**	**F (1, 36)**	**p**
Helper T lymphocyte (% $CD3^+$)	67.2 ± 15.1	61.5 ± 12.0	1.00	0.32
Cytotoxic T lymphocyte (% $CD3^+$)	27.9 ± 13.5	33.2 ± 10.6	0.92	0.35
B lymphocyte (% lymphocyte)	17.7 ± 8.3	12.2 ± 7.8	5.42	0.03
NK cell (% lymphocyte)	21.6 ± 11.3	27.5 ± 10.4	1.78	0.19
Regulatory T lymphocyte (% $CD4^+$)	2.1 ± 1.6	3.8 ± 2.3	7.89	0.008 *
† Age and sex were entered as covariates; Data are the mean ± SD. * Significant after correction for multiple statistical tests to avoid type I errors ($p < 0.01$ [0.05/5]); NK: Natural Killer				

Table 3: Percentages of circulating lymphocytes in patients and healthy control subjects.

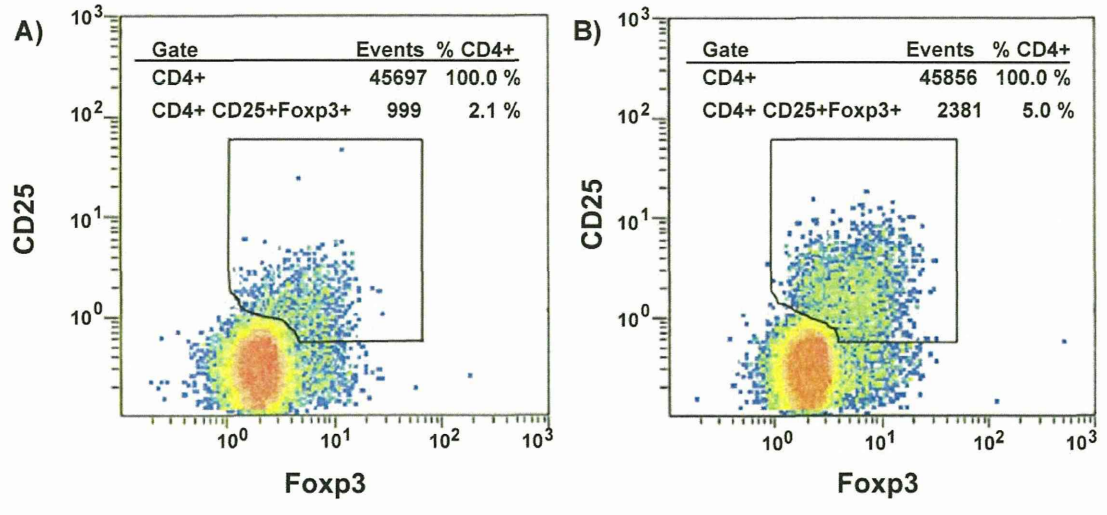

Figure 3: Flow cytometry analysis of the frequency of CD4+CD25+Foxp3+ cells within the CD4+ T-cell population. Representative plots are shown. The framed dots represent $CD4^+CD25^+Foxp3^+$ T cells (T_{regs}). The percentage of T_{regs} in patients (A) and controls (B) was 2.1% and 5.0%, respectively.

Lymphocyte subsets and their correlation with FA values in patients

The percentage of Tregs was significantly lower in patients than in healthy controls (Table 3). For patients and controls, representative flow cytometry analysis plots of the frequency of Tregs within the CD4+ T cell population are shown in Figure 3. Scatter plots depicting the percentage of Tregs in patients and controls are shown in Figure 4A. In patients, we found a significant positive relationship between the level of circulating Tregs and the FA value in the anterior limb of the internal capsule (r=0.50, p=0.04) (Figure 4B).

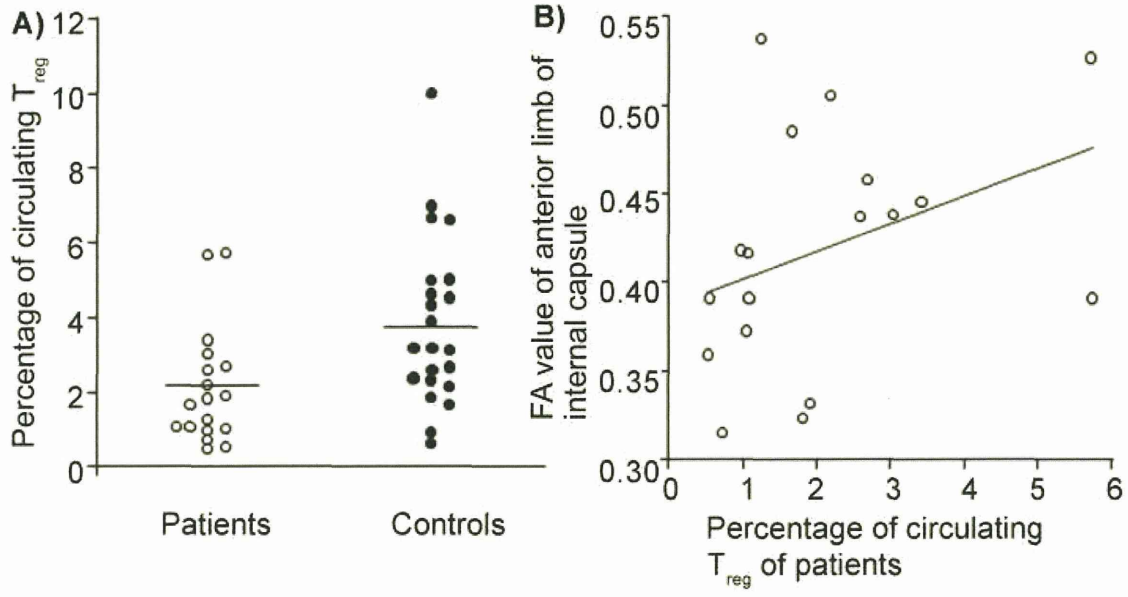

Figure 4: T_{reg} percentages in patients and controls and the relationship between the percentage of circulating Tregs and the FA value of the anterior limb of the internal capsule in patients. (A) The percentage of circulating Tregs differed significantly in the stoke patient and healthy control groups ($F1,36 = 7.89$, $p = 0.008$). (B) In stroke patients, a significant correlation was observed between the percentage of circulating T_{regs} and the FA value (r=0.50, p=0.04).

Discussion

Our findings showed that stroke patients had lower FA in the bilateral anterior limbs of the internal capsule when compared to healthy control subjects. The reduced FA in stroke patients was associated with decreased axial diffusivity. Axonal damage leads to a marked decrease in axial diffusivity, and demyelination leads to an increase in radial diffusivity [12]. Therefore, our finding of the reduced FA was a result not of demyelination but of a gross reduction in axonal number and/or size, possibly reflecting Wallerian degeneration secondary to neuronal loss due to stroke [13]. From an anatomical perspective, the anterior limb of the internal capsule represents the intercept point in the course of the frontal-subcortical circuits [14]; it has extensive connectivity with the cortical and subcortical areas. The reduced FA in the anterior limb of the internal capsule may reflect the conjunctive focus of degeneration due to stroke in spatially different sites of the cortical and subcortical areas [15].

Our results demonstrated that the percentage of circulating T_{regs} was lower in stroke patients than in healthy controls. The degree of reduction correlated with the decrease in the FA value in the internal capsule. This may indicate that a decrease in T_{regs} is associated with axonal damage in the internal capsule in stroke patients. After an ischemic stroke, activated T lymphocytes infiltrate the brain and function as a source of pro-inflammatory cytokines and cytotoxic substances [16-18]. However, not all T-cell subtypes are detrimental to acute stroke outcome, and there is evidence that T cells promote brain tissue repair and regeneration. T_{regs} are an important T-cell subtype; they support brain tissue repair and regeneration [19]. Infarct volume and neuronal dysfunction increased when mice were treated with an anti-CD25 monoclonal antibody to neutralize T_{regs} [20]. The ability of T_{regs} to protect the brain and improve stroke outcome was confirmed by Li et al. [21] who studied the effects of post-stroke T_{reg} therapy.

Although the interaction between the brain and the immune system subsequent to ischemic stroke has only recently been documented, the functional role of T_{regs} in other pathological conditions has been studied extensively. Most studies have ascribed the protective effect of T_{regs} to the alleviation of an excessive inflammatory response. It is reasonable to attribute the neuroprotective effect of T_{regs} in stroke to a similar mechanism [22].

T_{regs} limit the immune response by releasing IL-10, an anti-inflammatory cytokine [23]. In experimental brain ischemia with anti-CD25 monoclonal antibody-mediated depletion of T_{regs}, the addition of exogenous IL-10 reduced infarct volume [20]. T_{regs} also limit the immune response by releasing transforming growth factor-β, which may be required for neurogenesis [24]. In addition, T_{regs} conferred protection against stroke by blunting the increase in metalloproteinase-9 (MMP-9) [21]. Stroke-induced MMP-9 production resulting from neutrophil infiltration contributed to the breakdown of the blood-brain barrier and promoted leukocyte

infiltration and brain damage [25], whereas T_{reg} adoptive treatment inhibited MMP-9 production in the blood and the brain after ischemia [21].

The reason circulating T_{reg} levels were lower in stroke patients are not clear. People with lower levels of circulating T_{regs} may be more likely to develop stroke and experience severe axonal damage because the activity of their inflammatory system is excessive. Alternatively, the reduction in circulating T_{regs} after stroke may reflect the migration of T_{regs} to brain tissue for the repair of cerebral neuronal injuries. Our findings are based on cross-sectional data without immunohistochemical analysis, which limits our ability to determine which explanation is correct. However, our results are consistent with previous reports describing the brain-protective and outcome-improving effects of T_{regs}. Our findings raise the possibility that stroke outcome can be improved by targeting T_{regs} to protect the brain from tissue damage after stroke.

Whereas Liesz et al. [20] showed a protective effect of T_{regs} in stroke, Ren et al. [26] found that T_{regs} had no effect, and Kleinschnitz et al. [27] showed that T_{regs} exacerbated brain injury early after transient ischemia. However, the animal models used in the studies differed in several aspects, including the duration of ischemia and the methods for Treg depletion. In our study, the stroke patients predominantly suffered a modest ischemic insult, and their circulating lymphocytes were studied after 10–28 days. Differences in the severity and stage of ischemic insult may account for the conflicting results.

Our study has a few limitations. First, patients with significant comprehension deficits were excluded because clinical verbal interviews could not be conducted. Second, because our study was an *in vivo* human brain study, immunohistochemical analysis of brain tissue was not possible. Third, all of the patients took anti-coagulant/platelet medicine. Of note, 13 patients took acetylsalicylic acid, which has an anti-inflammatory effect and may have affected our results. However, the extent to which the results were affected by medication remains uncertain. Finally, we did not investigate the other functionally unique $CD4^+$ T-cell subsets (Th1, Th2, and Th17) in this study. A previous study reported that T_{regs}/Th17 cells were imbalanced in patients with cerebral infarction: the Th17 frequency increased, and the T_{reg} frequency decreased, relative to the balance in control subjects [28]. Th17 cells orchestrate tissue inflammation, whereas T_{regs} limit the immune response and prevent tissue damage. An imbalance between T_{regs} and Th17 cells in stroke patients may contribute to tissue damage [28]. Further analysis, taking these points into consideration, is needed to confirm our present findings.

In conclusion, the present study suggests that FA is reduced in the bilateral anterior limbs of the internal capsule in stroke patients. In addition, the percentage of circulating T_{regs} was reduced in stroke patients. The degree of reduction correlated with the decrease in the FA value in the internal capsule. T_{regs} might alleviate post-stroke white matter tissue damage by limiting the immune response. Further study of the role of T_{regs} in preventing post-stroke cerebral damage is needed.

Acknowledgments

This research was supported by the Japan Society for the Promotion of Science, Grant-in-Aid for Scientific Research (C), 24591740.

References

1. Donnan GA, Fisher M, Macleod M, Davis SM (2008) Stroke. Lancet 371: 1612-1623.
2. Magnus T, Wiendl H, Kleinschnitz C (2012) Immune mechanisms of stroke. Curr Opin Neurol 25: 334-340.
3. Iadecola C, Anrather J (2011) The immunology of stroke: from mechanisms to translation. Nat Med 17: 796-808.
4. Macrez R, Ali C, Toutirais O, Le Mauff B, Defer G, et al. (2011) Stroke and the immune system: from pathophysiology to new therapeutic strategies. Lancet Neurol 10: 471-480.
5. Craft TK, DeVries AC (2006) Role of IL-1 in poststroke depressive-like behavior in mice. Biol Psychiatry 60: 812-818.
6. Brait VH, Arumugam TV, Drummond GR, Sobey CG (2012) Importance of T lymphocytes in brain injury, immunodeficiency, and recovery after cerebral ischemia. J Cereb Blood Flow Metab 32: 598-611.
7. Brott T, Adams HP Jr, Olinger CP, Marler JR, Barsan WG, et al. (1989) Measurements of acute cerebral infarction: a clinical examination scale. Stroke 20: 864-870.
8. Goldstein LB, Samsa GP (1997) Reliability of the National Institutes of Health Stroke Scale. Extension to non-neurologists in the context of a clinical trial. Stroke 28: 307-310.
9. Folstein MF, Folstein SE, McHugh PR (1975) "Mini-mental state". A practical method for grading the cognitive state of patients for the clinician. J Psychiatr Res 12: 189-198.
10. Fazekas F, Chawluk JB, Alavi A, Hurtig HI, Zimmerman RA (1987) MR signal abnormalities at 1.5 T in Alzheimer's dementia and normal aging. AJR Am J Roentgenol 149: 351-356.
11. Kim DH, Adalsteinsson E, Glover GH, Spielman DM (2002) Regularized higher-order in vivo shimming. Magn Reson Med 48: 715-722.
12. Song SK, Yoshino J, Le TQ, Lin SJ, Sun SW, et al. (2005) Demyelination increases radial diffusivity in corpus callosum of mouse brain. Neuroimage 26: 132-140.
13. Thomalla G, Glauche V, Koch MA, Beaulieu C, Weiller C, et al. (2004) Diffusion tensor imaging detects early Wallerian degeneration of the pyramidal tract after ischemic stroke. Neuroimage 22: 1767-1774.
14. Axer H1, Keyserlingk DG (2000) Mapping of fiber orientation in human internal capsule by means of polarized light and confocal scanning laser microscopy. J Neurosci Methods 94: 165-175.
15. Yasuno F, Taguchi A, Yamamoto A, Kajimoto K, Kazui H, et al. (2014) Microstructural abnormalities in white matter and their effect on depressive symptoms after stroke. Psychiatry Res Neuroimaging.
16. Jander S, Kraemer M, Schroeter M, Witte OW, Stoll G (1995) Lymphocytic infiltration and expression of intercellular adhesion molecule-1 in photochemically induced ischemia of the rat cortex. J Cereb Blood Flow Metab 15: 42-51.
17. Yilmaz G, Arumugam TV, Stokes KY, Granger DN (2006) Role of T lymphocytes and interferon-gamma in ischemic stroke. Circulation 113: 2105-2112.
18. Brait VH, Jackman KA, Walduck AK, Selemidis S, Diep H, et al. (2010) Mechanisms contributing to cerebral infarct size after stroke: gender, reperfusion, T lymphocytes, and Nox2-derived superoxide. J Cereb Blood Flow Metab 30: 1306-1317.
19. Zouggari Y, Ait-Oufella H, Waeckel L, Vilar J, Loinard C, et al. (2009) Regulatory T cells modulate postischemic neovascularization. Circulation 120: 1415-1425.
20. Liesz A, Suri-Payer E, Veltkamp C, Doerr H, Sommer C, et al. (2009) Regulatory T cells are key cerebroprotective immunomodulators in acute experimental stroke. Nat Med 15: 192-199.
21. Li P, Gan Y, Sun BL, Zhang F, Lu B, et al. (2013) Adoptive regulatory T-cell therapy protects against cerebral ischemia. Ann Neurol 74: 458-471.
22. Xu X, Li M, Jiang Y (2013) The paradox role of regulatory T cells in ischemic stroke. ScientificWorldJournal 2013: 174373.
23. Chamorro Á, Meisel A, Planas AM, Urra X, van de Beek D, et al. (2012) The immunology of acute stroke. Nat Rev Neurol 8: 401-410.